2023-06-05

A high-dimensional microfluidic approach for selection of aptamers with programmable binding affinities

Chang, D

10.1038/s41557-023-01207-z
Nature Chemistry
Nature Research

A high-dimensional microfluidic approach for selection of aptamers with programmable binding affinities

Dingran Chang[1, *], Zongjie Wang[2, *], Connor D. Flynn[3,4], Alam Mahmud[5], Mahmoud Labib[1,4,6], Hansen Wang[1], Armin Geraili[1], Xiangling Li[1], Jiaqi Zhang[1], Edward H. Sargent[4,5,7,8] and Shana O. Kelley[1-4,8-10]

[1]Leslie Dan Faculty of Pharmacy, University of Toronto, Toronto, Ontario, Canada. [2]Department of Biomedical Engineering, McCormick School of Engineering, Northwestern University, Evanston, IL, USA. [3]Department of Chemistry, University of Toronto, Toronto, Ontario, Canada. [4]Department of Chemistry, Weinberg College of Arts & Sciences, Northwestern University, Evanston, IL, USA. [5]Department of Electrical and Computer Engineering, University of Toronto, Toronto, Ontario, Canada. [6]Peninsula Medical School, Faculty of Health, University of Plymouth, Plymouth, PL6 8BU, UK. [7]Department of Electrical and Computer Engineering, McCormick School of Engineering, Northwestern University, Evanston, IL, USA. [8]International Institute for Nanotechnology, Northwestern University, Evanston, IL, USA. [9]Department of Biochemistry, Feinberg School of Medicine, Northwestern University, Chicago, IL, USA. [10]Simpson Querrey Institute, Northwestern University, Chicago, IL, USA.
*These authors contributed equally.

e-mail: shana.kelley@northwestern.edu

Abstract

Aptamers are being applied as affinity reagents in analytical applications owing to their high stability, compact size, and amenability to chemical modification. Generating aptamers with different binding affinities is desirable but systematic evolution of ligands by exponential enrichment (SELEX), the standard for aptamer generation, is unable to quantitatively produce aptamers with desired binding affinities and requires multiple rounds of selection to eliminate false positive hits. Here we introduce Pro-SELEX, an approach for rapid discovery of aptamers with precisely defined binding affinities that combines efficient particle display, high-performance microfluidic sorting and high-content bioinformatics. Using the Pro-SELEX workflow, we were able to investigate the binding performance of individual aptamer candidates under different selective pressure in a single round of selection. Using human myeloperoxidase (MPO) as a target, we demonstrated that aptamers with dissociation constants spanning a twenty-fold range of affinities can be identified within one round of Pro-SELEX.

Introduction

Precise control over binding affinities between biomolecules is one of the critical means by which Nature allows thousands of types of biomolecules to operate in tandem with molecular-level control in heavily crowded environments. Moreover, molecules with well-defined binding affinities for a specific target – thus called affinity reagents – are essential for many applications, including biosensing, diagnostics, imaging, and therapeutics. For example, the binding affinity between a target analyte and its specific biorecognition element is the determinative factor that defines the dynamic range of a biosensor[1,2]. High-affinity recognition molecules with low dissociation constants (K_d) are sought for point-of-care applications to enable rapid binding events and low limits of detection. On the other hand, low-affinity reagents with fast association and dissociation rates have been used in real-time monitoring applications[3–5], because they can resolve the dynamic changes in their target analyte level. The advancement of detection modalities with extremely high resolution and low background levels has also made it possible for low-affinity binding reagents to achieve high detection sensitivity[2,6,7]. Hence, to meet the diverse requirements of different sensing scenarios, it is highly desirable to be able to generate recognition molecules with desired binding affinities against a specific target.

Nucleic acid aptamers have garnered significant interest as versatile affinity reagents and as promising alternatives to antibodies over the past three decades[8–10]. In recent years, aptamers have demonstrated great potential in real-time monitoring and wearable sensing applications[11–15]. Compared to antibodies, aptamers offer several unique features, including high stability, compact size, cost-effective mass synthesis, minimal batch-to-batch variation, non-immunogenic properties, and amenability to site-specific chemical modification[8,16,17]. Despite these attractive features, the use of aptamers in biosensing is relatively limited – one reason for this is a lack of high-quality aptamers for many biomolecular targets[16]. Conventional procedures for aptamer selection through SELEX are labor-intensive, time-consuming, and incapable of producing aptamers with programable binding affinities. A typical SELEX experiment requires 10-15 rounds of selection to allow the target-binding sequences to dominate the nucleic acid pool[16,18,19]. This inefficiency is due to the inability of traditional SELEX to separate aptamer candidates with diverse binding affinities in each round, as well as the introduction of undesired biases – such as PCR bias and amplification of parasitic sequences, through repeated rounds of selection. These factors also make the binding affinities of the selected aptamers unpredictable, requiring a number of sequences to be tested to identify an aptamer with desired properties.

Recent advancements in SELEX technologies with improved sequence partitioning efficiency, such as CE-SELEX[20], Non-SELEX[21], M-SELEX[22], and particle display

selection technology[23], have provided solutions for the aptamer selection challenge. However, none of these methods are able to quantitatively generate aptamers with defined binding affinities. Here we describe a new approach, referred to as Pro-SELEX, for quantitative isolation of aptamers with programable binding affinities. Our workflow consists of particle display, magnetic particle sorting, high-dimensional and parallelized selection, and high-content bioinformatics. Using this workflow, we are able to profile the binding performance of individual aptamer candidates at different target concentrations in a single round of selection. As a proof of concept, we selected aptamers specific to human myeloperoxidase (MPO), an emerging diagnostic and prognostic biomarker of coronary artery disease[24,25]. We successfully isolated a number of anti-MPO aptamers with pre-defined binding affinities (K_d) and developed algorithms relating selection data to this important biological parameter.

Results

The overall Pro-SELEX approach is summarized in Figure 1. Aptamer libraries displayed on particles are incubated with the binding target, where they are expected to bind to differing numbers of analyte molecules based on affinity. Magnetic nanoparticles are used to label the aptamer particles according to number of analyte molecules bound, and the aptamer particles are then sorted into different compartments of a microfluidic chip based on magnetic content. Pools of aptamers are generated based on the material collected in each compartment and sequenced. Comparative bioinformatics are employed to analyze the representation of individual aptamers and confirm the validity of sequences as true positive hits as well as infer relative affinity ranges.

Development of Pro-SELEX selection platform. To measure the relative affinity of each aptamer sequence in a nucleic acid library, particle display techniques[23] can be used to transform individual aptamer candidates from a solution-based aptamer library into monoclonal aptamer particles (APs) via emulsion PCR, where each particle presents many copies of a single nucleic acid sequence on its surface (Fig. 1a). The AP libraries can then be incubated with a specific target over a range of concentrations. Based on the Langmuir isotherm, the target binding level of an AP is dependent on the target concentration and the binding affinity of the aptamer coated on its surface, where half of the aptamer molecules will be bound to the target when the target concentration is equal to the K_d of the aptamer. APs with different binding levels can then be separated and collected using a high-resolution microfluidic sorting approach followed by sequencing analysis to identify aptamers with different binding affinities based on their binding performance at different target concentrations.

To accurately partition APs with different levels of target binding, we developed a magnetic labelling and microfluidic sorting approach (Fig. 1b). Polystyrene particles (7 μm in diameter) were used to prepare APs. After incubation of APs with a biotinylated target of interest, the particles were labelled with anti-biotin magnetic nanoparticles (MNPs, 50 nm in diameter) to convert the target binding into a magnetic content. The labelled mixture was then sorted and isolated using a microfluidic device (Pro-SELEX chip). This device features four capture zones with differing linear velocities to allow differential sorting of APs with varying levels of magnetic content. Owing to the low magnetic susceptibility of MNPs, each capture zone contains microfabricated structures to create localized regions of low flow velocity and enhanced capture dynamics (Supplementary Fig. 1). The first zone exhibits the highest linear velocity and thus retains APs with high magnetic content, as the retaining magnetic force overcomes the drag force exerted by the high flow velocity. The ensuing three zones exhibit gradually reduced linear velocities (Fig. 1c for simulation information and Fig. 1d). This design allows APs to be separated and captured in different zones according to their target binding levels. We demonstrated that the Pro-SELEX chip is able to sort the particles based on their magnetic content (Fig. 1e and Supplementary Fig. 2). It is worth noting that the stringency and resolution of magnetic separation of the Pro-SELEX chip are programable by adjusting the chip flow rate (Fig. 1e). Similar device design has been used to perform profiling of cellular proteins and nucleic acids as well as rare cell capture, demonstrating superior throughput and recovery rate compared to fluorescence-activated cell sorting (FACS) and magnetic-activated cell sorting (MACS)[26–29]. We now demonstrate the utility of this type of device for aptamer selection.

Validation of the sorting performance of Pro-SELEX chip. In the first suite of experiments, we used thrombin aptamers as a test case to validate the approach (Fig. 2a). We first tested whether the Pro-SELEX chip could sort APs with different levels of target binding. Thrombin-03 aptamer[23]-coated particles (03-particles) with varying target binding levels were prepared by incubating the particles with a range of thrombin concentrations, from 1 pM to 1 nM, followed by labelling with MNPs (Fig. 2b). These 03-particles were then sorted using Pro-SELEX chips at flow rates of 8 mL/hr and 16 mL/hr and distinctive sorting profiles were generated (Fig. 2c and 2d). The particles with high magnetic content (1 nM and 100 pM) were primarily captured in zone 1 of the chip at a flow rate of 8 mL/hr and partially shifted to zone 2 upon increasing the flow rate to 16 mL/hr, whereas particles with lower magnetic content were mainly collected in later zones and almost all of the non-target bound particles were detected in the waste. This observation indicates that the Pro-SELEX chip is able to sort and capture APs based on their target binding levels, employing several flow rates to stratify the sorting profile.

Next, we explored whether the Pro-SELEX approach could separate APs with different binding affinities. Two types of APs were prepared carrying comparable copy numbers of either Thrombin-03 (K_d 7.04 pM) or Thrombin-TBA (K_d 2.6 nM) [23,30] (Supplementary Fig. 3). Both APs together with primer-coated particles were tested with three thrombin concentrations and analysed using flow cytometry (Figs. 2e-g) and the Pro-SELEX chip (Figs. 2h-j). When using a thrombin concentration of 1 μM, which is significantly higher than the K_d of both aptamers, both APs became saturated by the target and were captured in zone 1 of the chip. When the target concentration dropped to 1 nM, a significant separation was observed such that the high-affinity 03-particles remained in zone 1 and the low-affinity TBA-particles were binned in zones 2 and 3. When the target concentration further decreased to 1 pM, most TBA-particles were collected in the waste

whereas a significant fraction of the 03-particles were still captured in the chip. Notably, less than 0.5% of the primer-coated particles were captured by the chip at a flow rate of 8 mL/hr regardless of the thrombin concentrations, showcasing the high capture specificity of the Pro-SELEX chip. We further investigated the effect of flow rate on the nonspecific capture of aptamers to ensure that nonbinders can efficiently be removed during the selection process (Supplementary Fig. 4). Together, these results demonstrated that the Pro-SELEX chip is capable of separating APs with distinctive binding affinities, where target concentrations play a prominent role in determining the separation efficiency.

Selection of MPO aptamers using Pro-SELEX. We next explored whether we could use the Pro-SELEX platform to efficiently generate aptamers. We selected MPO as the model target for testing the capability of Pro-SELEX for aptamer selection. An initial random DNA library containing ~10^{14} random DNA molecules was first subjected to a pre-enrichment step consisting of 3 rounds of both counter selections against undesired targets and conventional SELEX towards MPO immobilized beads to remove nonspecific binders and reduce the sequence space of the library (Supplementary Table 1 and Fig. 5). The enriched library was then used as a template to prepare AP libraries through emulsion PCR (Supplementary Fig. 6). The AP libraries were tested at five MPO concentrations (10 pM, 100 pM, 1 nM, 10 nM, and 100 nM), in an attempt to isolate aptamers with K_d within this range. It was critical to ensure that the MPO molecules were available in excess and not depleted during the target incubation, especially when testing low target concentrations, to confirm that the binding between APs and MPO follows the Langmuir isotherm (See Supplementary Table 2). AP libraries were then sorted by Pro-SELEX chips at two flow rates, 16 mL/hr and 32 mL/hr (Fig. 3a). It required less than 20 minutes for the Pro-SELEX chip to sort 5×10^7 APs, which is faster than the FACS-based

sorting method[23]. Particles captured by each zone within the ten chips were then collected (Fig 3 b and c). As expected, we clearly observed that the fractions of APs captured by Pro-SELEX chips decreased upon lowering the target concentration and the sorting profiles of the APs libraries were shifted when using a faster flow rate, highlighting the high resolution of our approach.

The particles collected from zones 1-3 of each chip together with the unsorted aptamer population, for a total of 31 DNA pools, were subjected to high-throughput sequencing (HTS). We also created a scoring tool, AptaZ, which was employed to comprehensively analyse the fold of enrichment of each aptamer candidate from 30 DNA pools and generate a Z score (see details in Supporting discussion and Fig. 3d). Aptamer candidates that can survive multiple target concentrations, especially low concentrations at two flow rates and be repeatedly captured by the chips would generate high Z scores (Fig. 3e). Eight MPO aptamer candidates, MPO-01 to MPO-08, with diverse Z scores were randomly chosen for characterization (Supplementary Table 3). All eight aptamers demonstrated an affinity for MPO with K_d values ranging from 227 pM to 27.8 nM (Fig. 3f and Supplementary Fig. 7). A linear relationship was observed between the K_d values of the 8 candidates and their calculated Z scores based on curve fitting (Fig. 3g), indicating the potential of using Z scores to search for the aptamer candidates with desired binding affinities.

Quantitative selection of MPO-aptamers with desired affinities. We next explored whether the Z score could be used to quantitatively screen aptamers with desired binding affinities. A search band was generated based on the correlation between the Z score and the K_d values of the validated MPO aptamers (Fig.4 a). We set the desired K_d values as 1000 pM, 3000 pM, 9000 pM, and 27,000 pM and calculated their theoretical Z score ranges based on the search band. Aptamer candidates within this range were then chosen and examined for their binding affinities, and the differences between their experimental K_d and the desired K_d were calculated. We defined a difference smaller than 25% as a “great fit”.

By evaluating the binding affinity of multiple MPO aptamer candidates in different Z score ranges (Supplementary Fig. 8 and Table 4), we found that the success rate in identifying a “great fit” was between 20%-50%, suggesting that by testing no more than five aptamer candidates within the Z score range, we can identify one aptamer with the desired binding affinity (Fig. 4b). The “best fits” for the requested affinities are MPO-14 with K_d of 897 pM, MPO-18 with K_d of 3192 pM, MPO-25 with K_d of 8778 pM, and MPO-34 with K_d of 24910 pM (Fig. 4c, their secondary structures are provided in Supplementary Fig. 9). The K_d values of the tested aptamers spanning more than 100-fold. The selected aptamers also demonstrated excellent specificities for MPO (Supplementary Fig. 10) as well as the

potential to be used to analyse biological samples (Supplementary Fig. 11). MPO-16 revealed the highest binding affinity (K_d =166 pM) and its sequence, secondary structure, binding specificity and binding performance in biological samples have been highlighted in Supplementary Fig. 12. It should be noted that the normal MPO level from a healthy middle-aged population has been reported to be <640 pM, with higher MPO levels being associated with increased risk of cardiovascular diseases[31]. We believe that the anti-MPO aptamers with different binding affinities reported here will become valuable tools in future MPO monitoring applications.

Discussion

We developed an aptamer generation method, Pro-SELEX, which enables efficient and quantitative generation of aptamers with desired binding affinities. Unlike conventional SELEX methods that rely on iterative rounds of selection to screen for aptamer candidates (Fig. 5a), our approach monitors the binding performance of individual aptamer candidates at different target concentrations in a single round of selection (Fig. 5b), taking advantage of the high level of parallelization enabled by high-dimensional microfluidics. Current iterations of SELEX, such as CE-SELEX and particle-based display, despite their significantly improved efficiency in generating aptamers, still select for aptamers with the highest affinities (Fig. 5c). Unfortunately, high-affinity aptamers might not be suitable for all applications. For instance, affinity receptors with suitable K_d should be selected based on the target concentration range to achieve quantitative biomolecular recognition, as the dynamic range of single-site binding typically spans 81-fold changes in target concentrations which is dependent on the K_d of receptors[2]. If the K_d of a receptor is significantly lower than the relevant concentration range, the resulting saturated signal will not change over the detection range[2]. A strategy to manipulate the dynamic range of sensing is to combine receptors with different target affinities[1,32]. This naturally raises the demand to generate aptamers with different K_d. In addition, lower-affinity receptors with fast binding kinetics (high on-rate and off-rate) are ideal for continuous monitoring as they allow for rapid equilibration with the surrounding target[4,33]. The development of sophisticated detection modalities in recent years with considerably lower levels of background and digital outputs makes it possible to quantify molecules in log dynamic ranges at concentrations much lower than K_d[34–36]. By exploiting these types of sensing mechanisms, low-affinity receptors can also achieve high detection sensitivity. Collectively, it will be advantageous to have the capability of generating receptors with customizable binding affinities to meet the requirements of diverse applications. The Pro-SELEX platform was developed to fulfill this need.

The Pro-SELEX approach is also highly programable and can be easily customized to suit various other applications. For example, the particle size used in this platform is large

enough (7 μm in diameter) to capture a wide range of targets, from small molecules to viruses or bacteria. Given the high efficiency of Pro-SELEX and the broad applications of aptamers during the SARS-CoV-2 pandemic[37–39], our platform can be applied for rapid generation of anti-virus aptamers during the early stage of a pandemic. The time required for Pro-SELEX and SELEX has been summarized in Supplementary Table 5. In addition, recent advances in incorporating non-natural nucleotides with diverse structures and functional groups into aptamers would enable aptamers with enhanced binding performance and expanded target range[40–43]. We believe our approach can be adapted to accommodate these unnatural nucleotides to efficiently produce modified aptamers.

Acknowledgement

This research was supported in part by the Canadian Institutes of Health Research (grant no. FDN-148415) and the Collaborative Health Research Projects Program (CIHR/NSERC partnered). This research is part of the University of Toronto's Medicine by Design initiative, which receives funding from the Canada First Research Excellence Fund. This research was supported in part by the McCormick Catalyst Fund at Northwestern University.

Author contributions

D.C, Z.W, and S.O.K conceived and designed the experiments. D.C performed the aptamer selection and validation. Z.W performed the chip fabrication and wrote the code for AptaZ. All authors discussed the results, analyzed the data, and contributed to the preparation and editing of the manuscript.

Competing interests

S.O.K is an inventor on a patent entitled "Device for capture of particles in a flow" US10073079 that licensed to CTRL Therapeutics. The remaining authors declare no competing interests.

Figure Legends/Captions

Figure 1. *Quantitative isolation of aptamers with different binding affinities via a high-dimensional microfluidic approach.* **a**, Overall workflow. **b**, Isolation of aptamer particles with different levels of target binding using Pro-SELEX chips. **c**, Separation rationale. Simulated linear flow velocity profile. Formation of capture pockets was observed in the valley of X-shaped microstructures. **d**, Magnitude of linear flow velocity. **e**, Determination of the median magnetic load of particles captured by Pro-SELEX at different flow rates (8 mL/hr, 16 mL/hr, and 32 mL/hr. Data are presented as mean values, and the error bars represent the standard deviation of three replicates. W represents particles collected from outlet (waste).

Figure 2. *Validation of the sorting performance of the Pro-SELEX chip using anti-thrombin aptamers with different binding affinities.* **a**, Workflow of the validation

experiments. **b***,* Evaluation of the binding performance of thrombin-03 coated aptamer particles at thrombin concentrations of 1 nM, 100 pM, 10 pM, 1 pM and 0 pM. The particles are labelled with MNPs and anti-MNPs labelling check reagent-APC and analyzed by flow cytometry. **c-d**, Determination of the capture profile of particle-displayed thrombin-03 aptamer prepared using different thrombin concentrations at flow rates of 8 and 16 mL/hr. Data are presented as mean values, and the error bars represent the standard deviation of three replicates. **e-g**, Analysis of particle-displayed thrombin aptamer 03, TBA and a primer sequence after incubation with 1 μM **(e),** 1 nM **(f)** and 1 pM **(g)** thrombin molecules. The particles are labelled with MNPs and anti-MNPs labelling check reagent-APC and analyzed by flow cytometry. **h-j**, Sorting of the particle-displayed thrombin aptamers 03, TBA and a primer sequence using Pro-SELEX chip at a flow rate of 8 mL/hr. Data are presented as mean values, and the error bars represent the standard deviation of three replicates.

Figure 3. *Isolation of anti-MPO aptamers with different binding affinities via a high-dimensional microfluidic-based approach.* **a**, Workflow of the selection experiments. Five MPO concentrations (100 nM, 10 nM, 1 nM, 100 pM, and 10 pM) were tested at flow rates of 16 and 32 mL/hr for the screening experiments. Particles were collected from individual capture zones (z1-z3) and analyzed by high-throughput sequencing and the AptZ tool for aptamer identification. **b-c**, Aptamer particles collected from z1-z4 of Pro-SELEX chips at flow rates of 16 mL/hr **(b)** and 32 mL/hr **(c)**. **d**, Distribution of calculated z score over the pool of sequences presented in MPO selection. **e**, The heatmap of fold of enrichment in all 30 conditions of sequences with different Z scores. The AptaZ algorithm comprehensively considers the fold of enrichment from different conditions to generate Z scores to quantitatively rank aptamers. **f**, Eight candidates with different Z scores were expressed on particles and incubated with Cy5-labeled MPO prior to analysis via flow cytometry. Each line represents a fitted Langmuir isotherm. Data are presented as mean values, and error bars represent the standard deviation of three replicates. **g**, The relationship between calculated Z score and validated K_d derived from the eight candidates was examined. The Z score correlates with the K_d value in a linear fashion according to curve fitting.

Figure 4. *Quantitative isolation of anti-MPO aptamers with desired affinities based on their Z score.* **a**, Strategy for validation. A K_d search band was generated based on the K_d-Z score curve fit. The Z score ranges of four desired K_d (1000 pM, 3000 pM, 9000 pM and 27,000 pM) were calculated. Several aptamer candidates within the Z score ranges can be tested and the difference between their actual K_d and the desired K_d can then be calculated to evaluate the accuracy of Z core-based aptamer identification. **b**, Evaluation of the accuracy of using Z scores to identify MPO aptamers with K_d values of 1000 pM, 3000 pM, 9000 pM and 27,000 pM. The red dots represent the aptamers with actual K_d <25% difference from the desired K_d. The data points of MPO-13 (K_d:9580 pM) and APO-27 (K_d:27700 pM) are outside their axis limits and not shown. **c**, The binding curve of the best-fit aptamer candidates. Polystyrene particles coated with aptamers, MPO-14, MPO-18, MPO-25, or MPO-34 were incubated with Cy-5 labelled MPO prior to analysis via flow

cytometry. The red line represents the results of fitting a Langmuir binding isotherm to the MPO binding data. Error bars represent the standard deviation of three replicates, and centres of error bars represent mean values.

Figure 5. *Comparison of Pro-SELEX with current aptamer selection technologies.* **a**, Conventional SELEX strategy. **b**, Pro-SELEX strategy. **c**, A table summarizing the performance criteria of Pro-SELEX versus current aptamer selection technologies.

References

1. Drabovich, A. P., et al. Smart Aptamers Facilitate Multi-Probe Affinity Analysis of Proteins with Ultra-Wide Dynamic Range of Measured Concentrations. J. Am. Chem. Soc. **129**, 7260–7261 (2007).
2. Wilson, B. D. et al. Re-Evaluating the Conventional Wisdom about Binding Assays. *Trends Biochem. Sci.* **45**, 639–649 (2020).
3. Arroyo-Currás, N. et al. Real-time measurement of small molecules directly in awake, ambulatory animals. *Proc. Natl. Acad. Sci. U.S.A.* **114**, 645–650 (2017).
4. Fercher, C. et al. Recombinant Antibody Engineering Enables Reversible Binding for Continuous Protein Biosensing. *ACS Sens.* **6**, 764–776 (2021).
5. Plaxco, K. W. et al. Seconds-resolved, in situ measurements of plasma phenylalanine disposition kinetics in living rats. *Anal. Chem.* **93**, 4023–4032 (2021).
6. Xue, L. et al. Solid-state nanopore sensors. *Nat. Rev. Mater.* **5**, 931–951 (2020).
7. Sevenler, D. et al. Beating the reaction limits of biosensor sensitivity with dynamic tracking of single binding events. *Proc. Natl. Acad. Sci. U.S.A.* **116**, 4129–4134 (2019).
8. Wang, T. et al. Three decades of nucleic acid aptamer technologies: Lessons learned, progress and opportunities on aptamer development. *Biotechnol. Adv.* **37**, 28–50 (2019).
9. Liu, J. et al. Functional nucleic acid sensors. *Chem. Rev.* **109**, 1948–1998 (2009).
10. Song, S. et al. Aptamer-based biosensors. *Trends Anal. Chem.* **27**, 108–117 (2008).
11. Wang, B. et al. Wearable aptamer-field-effect transistor sensing system for noninvasive cortisol monitoring. *Sci. Adv.* **8**, 967 (2022).
12. Nakatsuka, N. et al. Aptamer–field-effect transistors overcome Debye length limitations for small-molecule sensing. *Science* **362**, 319–324 (2018).
13. Mage, P. L. et al. Closed-loop control of circulating drug levels in live animals. *Nat. Biomed. Eng.* **1**, 1–10 (2017).
14. Ferguson, B. S. et al. Real-time, aptamer-based tracking of circulating therapeutic agents in living animals. *Sci. Transl. Med.* **5**, 213ra165 (2013).
15. Zhao, C. et al. Implantable aptamer-field-effect transistor neuroprobes for in vivo neurotransmitter monitoring. *Sci. Adv.* **7**, 7422 (2021).

16. Qian, S. et al. Aptamers from random sequence space: Accomplishments, gaps and future considerations. *Anal. Chim. Acta* **1196**, 339511 (2022).

17. Li, F. et al. Aptamers facilitating amplified detection of biomolecules. *Anal. Chem.* **87**, 274–292 (2015).

18. Ellington, A. D. et al. In vitro selection of RNA molecules that bind specific ligands. *Nature* **346**, 818–822 (1990).

19. Tuerk, C. et al. Systematic evolution of ligands by exponential enrichment: RNA ligands to bacteriophage T4 DNA polymerase. *Science* **249**, 505–510 (1990).

20. Mendonsa, S. D. et al. In Vitro Evolution of Functional DNA Using Capillary Electrophoresis. *J. Am. Chem. Soc.* **126**, 20–21 (2004).

21. Berezovski, M. et al. Non-SELEX selection of aptamers. *J. Am. Chem. Soc.* **128**, 1410–1411 (2006).

22. Lou, X. et al. Micromagnetic selection of aptamers in microfluidic channels. *Proc. Natl. Acad. Sci. U.S.A.* **106**, 2989–2994 (2009).

23. Wang, J. et al. Particle display: a quantitative screening method for generating high-affinity aptamers. *Angew. Chem. Int. Ed.* **53**, 4796–4801 (2014).

24. Zhang, R. et al. Association Between Myeloperoxidase Levels and Risk of Coronary Artery Disease. *JAMA* **286**, 2136–2142 (2001).

25. Baldus, S. et al. Myeloperoxidase Serum Levels Predict Risk in Patients With Acute Coronary Syndromes. *Circulation* **108**, 1440–1445 (2003).

26. Labib, M. et al. Single-cell mRNA cytometry via sequence-specific nanoparticle clustering and trapping. *Nat. Chem.* **10**, 489–495 (2018).

27. Labib, M. et al. Tracking the expression of therapeutic protein targets in rare cells by antibody-mediated nanoparticle labelling and magnetic sorting. *Nat. Biomed. Eng.* **5**, 41–52 (2021).

28. Wang, Z. et al. Efficient recovery of potent tumour-infiltrating lymphocytes through quantitative immunomagnetic cell sorting. *Nat. Biomed. Eng.* **6**, 108–117 (2022).

29. Wang, Z. et al. Ultrasensitive Detection and Depletion of Rare Leukemic B Cells in T Cell Populations via Immunomagnetic Cell Ranking. *Anal. Chem.* **93**, 2327–2335 (2021).

30. Bock, L. C. et al. Selection of single-stranded DNA molecules that bind and inhibit human thrombin. *Nature* **355**, 564–566 (1992).

31. Tang, W. H. W. et al. Usefulness of Myeloperoxidase Levels in Healthy Elderly Subjects to Predict Risk of Developing Heart Failure. *Am. J. Cardiol.* **103**, 1269 (2009).

32. Vallée-Bélisle, A. et al. Engineering biosensors with extended, narrowed, or arbitrarily edited dynamic range. *J. Am. Chem. Soc.* **134**, 2876–2879 (2012).

33. Tu, J. et al. The Era of Digital Health: A Review of Portable and Wearable Affinity Biosensors. *Adv. Funct. Mater.* **30**, 1906713 (2020).

34. Deng, R. et al. Recognition-Enhanced Metastably Shielded Aptamer for Digital Quantification of Small Molecules. *Anal. Chem.* **90**, 14347–14354 (2018).

35. Das, J. et al. Reagentless biomolecular analysis using a molecular pendulum. *Nat. Chem.* **13**, 428–434 (2021).

36. Wang, L. et al. Rapid and ultrasensitive electromechanical detection of ions, biomolecules and SARS-CoV-2 RNA in unamplified samples. *Nat. Biomed. Eng.* **6**, 276–285 (2022).

37. Zhang, Z. et al. High-Affinity Dimeric Aptamers Enable the Rapid Electrochemical Detection of Wild-Type and B.1.1.7 SARS-CoV-2 in Unprocessed Saliva. *Angew. Chem. Int. Ed.* **60**, 24266–24274 (2021).

38. Li, J. et al. Diverse high-affinity DNA aptamers for wild-type and B.1.1.7 SARS-CoV-2 spike proteins from a pre-structured DNA library. *Nucleic Acids Res.* **49**, 7267–7279 (2021).

39. Yang, G. et al. Identification of SARS-CoV-2-against aptamer with high neutralization activity by blocking the RBD domain of spike protein 1. *Signal Transduct. Target. Ther.* **6**, 227 (2021).

40. Lapa, S. A. et al. The Toolbox for Modified Aptamers. *Mol. Biotechnol.* **58**, 79–92 (2016).

41. Gawande, B. N. et al. Selection of DNA aptamers with two modified bases. *Proc. Natl. Acad. Sci. U.S.A.* **114**, 2898–2903 (2017).

42. Gordon, C. K. L. et al. Click-Particle Display for Base-Modified Aptamer Discovery. *ACS Chem. Biol.* **14**, 2652–2662 (2019).

43. Pfeiffer, F. et al. Identification and characterization of nucleobase-modified aptamers by click-SELEX. *Nat. Protoc.* **13**, 1153–1180 (2018)

Methods

Materials. Carboxyl polystyrene particles (7 µm, #PC06004) were purchased from Bangs Laboratories, Inc. DPBS (#14190250), streptavidin (Cy5, #SA1011), Dynal MyOne C1 streptavidin dynabeads (65001), biotinylated peroxidase (#432040), PureLink™ Quick Gel Extraction Kit (K210012), EZ-Link™ Micro NHS-PEG4-biotinylation Kit(#21955) and dNTP Mix(#R0192) were ordered from Thermo Fisher Scientific. Light mineral oil (#M5310), 2-butanol (#294810), N-(3-dimethylaminopropyl)-N′-ethylcarbodiimide hydrochloride (EDC, #161462), N-hydroxysuccinimide (NHS, #130672), Human serum (H4522-100ML) and imidazole hydrochloride (#13386) were purchased from Sigma Aldrich. Anti-biotin microbeads ultrapure (#130-105-637) and Labeling Check Reagents-APC (#130-122-219) were purchased from Miltenyi Biotech. Recombinant Human myeloperoxidase protein (MPO, 3174-MP-250) was ordered from R&D Systems. Lambda exonuclease (#M0262S) was ordered from New England Biolabs (NEB). GoTaq G2 Hot Start Taq Polymerase (#M7405) was purchased from Promega. ABIL® EM 90 was obtained from Evonik. Recombinant Human BNP protein (#ab87200) and recombinant human RANTES protein (#ab269212) were ordered from Abcam. Biotinylated thrombin (#69723)

was obtained from Fisher Scientific. DT-20-M Gamma tubes were ordered from IKA Works. Water was purified with a Millipore Milli-Q Biocel water purification system.

All DNA oligonucleotides (see table S1) were obtained from Integrated DNA Technologies and purified by 10% denaturing (8 M urea) polyacrylamide gel electrophoresis (dPAGE), and their concentrations were determined by NanoDrop spectrophotometer. The library was 90-nt long, consisting of a 50-nt variable region flanked by two 20-nt primer sites (5'-AGCAGCACAGAGGTCAGATG-N50-AAGTGTAGTGTCTCCGTGGC-3'). The Forward primer (FP) sequence was 5'-AGCAGCACAGAGGTCAGATG-3' and the reverse primer (RP) was 5'-GCCACGGAGACACTACACTT-3'. The sequencing adaptors were 5'-ACACTCTTTCCCTACACGACGCTCTTCCGATCT-NNNN-AGCAGCACAGAGGTCAGATG-3' for the FP adaptor and 5'-GTGACTGGAGTTCAGACGTGTGCTCTTCCGATCTGCCACGGAGACACTACACTT-3' for the RP adaptor.

Chip fabrication and operation. The microfluidic device was fabricated using the protocol combining 3D printing and soft lithography techniques, as described before[44]. In brief, the master mold was manufactured by a stereolithographic 3D printer (Microfluidics Edition 3D Printer, Creative CADworks, Canada) using the "CCW master mold for PDMS" resin (Resinworks 3D, Canada) with a layer thickness of 50 μm. The actual chips were fabricated by casting polydimethylsiloxane (PDMS, Sylgard 184, Dow Chemical, US) on the printed molds, followed by 120-min incubation at 70 ^{o}C for curing. Cured PDMS replicas were peeled off, punched and plasma bonded to no.1 glass thickness coverslips (260462, Ted Pella, US) to finish the chip. Before use, the chips were conditioned by a binding buffer (DPBS with 2.5 mM $MgCl_2$, 1 mM $CaCl_2$, 0.01% TWEEN-20) to remove air bubbles. During operation, each chip was attached to arrayed N52 NdFeB magnets (D14-N52, K&J Magnetics, US) and fluidically connected to a digital syringe pump (Fusion 100, Chemyx, US) under the withdrawn mode.

Finite element simulation. Numerical simulation of the flow velocity pattern within the microfluidic device was carried out by COMSOL Multiphysics (Version 5.6, COMSOL Inc., Sweden) using the 3D creeping flow module. The key parameters for simulation were set as below: boundary condition: pressure of 0 Pa with suppression of backflow, wall condition: no slip, and mesh size: physics-controlled, fine.

Scanning electron microscopy. Fabricated chips were coated with 15 nm Au using a desktop sputter coater (Denton Desk II, Leica, Germany). Coated chips were imaged under a field-emission scanning electron microscope (SU5000, Hitachi, Japan) using 5kV accelerating voltage and high-vacuum mode.

Preparation of biotin labelled protein targets. MPO protein as well as proteins used for counter selection, including human serum proteins, BNP and RANTES, were biotinylated using the EZ-Link Micro NHS-PEG4-Biotinylation Kit (Thermo Fisher Scientific). The free biotin was removed by Zeba Desalt Spin Column with 7K molecular weight cut off (10 mL, Thermo Fisher Scientific). We measured biotinylated MPO protein concentration based on absorbance at 280 nm using a NanoDrop spectrophotometer.

Pre-enrichment by SELEX. The DNA library (6 x 10^{14} random DNA molecules) was diluted with 1 mL of binding buffer and heated at 90°C for 1 min, followed by annealing at room temperature for 10 min. Then, a mixture of magnetic beads (Dynabeads MyOne streptavidin C1, Thermo Fisher Scientific) conjugated with human serum proteins, thrombin, BNP and RANTES were

washed twice with binding buffer, and incubated with the DNA library at room temperature (RT) for 2 hrs. The DNA in the supernatant was collected, mixed with MPO (R&D Systems)-conjugated magnetic beads, and incubated at RT for 1 hr. The beads were washed five times with 500 µL of binding buffer. The MPO-bound DNA molecules were then eluted by adding 100 µL water and heating at 95°C for 15 minutes. The eluted DNA was PCR amplified and used for the following round of enrichment and aptamer particle synthesis. Three rounds of pre-enrichment were performed to remove both nonspecific DNA molecules that bind to other protein targets and inactive DNA molecules that do not bind to MPO protein.

Preparation of forward primer particles. 1 mL of 7-µm carboxyl polystyrene particles (Bangs Laboratories) were washed once with 1 mL of 0.01 N NaOH and three times with 1 mL of nuclease-free water, then resuspended in a 500 µL reaction mixture containing 200 mM NaCl, 0.2 mM 5'-amino-modified FP (or amino-modified thrombin aptamers), 1 mM imidazole chloride, and 250 mM EDC (Sigma Aldrich). The free carboxyl on the particles were then converted into amino-reactive NHS-ester in the presence of 250 mM EDC and 100 mM NHS in 2-(**N**-morpholino)ethanesulfonic acid (MES) buffer (100 mM, PH 4.7) (Thermo Scientific) for 30 minutes at RT. The particles were then conjugated with 20 mM amino-PEG12 (Thermo Scientific) in MES buffer for one hour. The particles were washed three times with 1 mL of TE (10 mM Tris, pH 8.0, 0.1 mM EDTA), suspended in 1 mL of TE buffer, and stored at 4 °C.

Preparation of aptamer particles. *Emulsion PCR:* The oil phase (prepared fresh each time) was composed of 3% ABIL®EM90, and 0.05% Triton X-100 in mineral oil. The aqueous phase consisted of 1× GoTaq PCR buffer (Promega), 25 mM $MgCl_2$, 3.5 mM of each dNTP (Therm Fisher Scientific), 3 µM 5' phosphorylated reverse primer (Phos-RP), 0.5 U/µl of GoTaq Hot Start Polymerase (Promega), 2 pM template DNA, and 5×10^7 FP-coated particles in a total volume of 1 mL. Water-in-oil emulsions were prepared by adding 1 mL of the aqueous phase to 7 mL of the oil phase in a DT-20 tube (IKA) locked into the Ultra-Turrax Device (IKA). This addition was performed dropwise over 30 seconds while the mixture was stirred at 650 rpm in the Ultra-Turrax. After adding the aqueous phase, we continued stirring the mixture for 5 min. The emulsions were distributed in 100 µl aliquots into ~80 wells of a 96-well PCR plate. We performed PCR under the following cycling conditions: 94 °C for 3 min, followed by 50 cycles of 94 °C for 15 sec, 58 °C for 30 sec and 72 °C for 60 sec. *Emulsion PCR cleanup:* After PCR, each PCR well was mixed with 50 µl of 2-butanol to break the emulsion. The broken emulsions were then transferred to a 50 mL tube. Next, 150 µl of 2-butanol were added to each PCR well to collect the leftover emulsions and transferred to the 50 mL collection tube. After vortexing for 30 sec, the particles were pelleted by centrifugation at 2,500 × *g* for 5 min. After carefully removing the oil phase, we resuspended the particles in 1 mL of emulsion breaking (EB) buffer (100 mM NaCl, 1% Triton X-100, 10 mM Tris-HCl, pH 7.5, and 1 mM EDTA) and transferred them to a new 1.5 mL tube. After vortexing for 30 sec and centrifugation for 90 sec at 15,000 × *g*, we removed the supernatant. Particles were then washed three times with TE buffer by centrifugation followed by resuspension in 500 µl TE. *Single strand generation:* To generate single-stranded DNA, we first removed the supernatant by countrification. We then treated the particles with 100 U of Lambda exonuclease (NEB) in 500 µl of reaction buffer (67 mM glycine-KOH (pH 9.4), 2.5 mM $MgCl_2$, 0.01% (v/v) Triton X-100.) at 37 °C for 1 hour, following by inactivation of the reaction by heating at 80°C for 15 min. The particles were then washed three times with 1 mL of TE buffer, suspended in 1 mL of TE buffer and stored at 4 °C.

Aptamer particle (AP) quality control. *Forward primer conjugation:* To test the conjugation efficiency of the forward primers, we incubated 1 μM Cy5-labeled FP complementary sequence (Cy5-FP') with 1 μL of FP particles in 100 μL of binding buffer at 60 °C for 10 minutes, then cooled down at room temperature for 10 minutes. The particles were washed twice with 100 μL binding buffer and analysed with a Cytoflex flow cytometer (Beckman Coulter Life Science). Acquired data were analysed using FlowJo software (version 10.8.1, FlowJo). *Aptamer particle monoclonality:* Based on the Poisson distribution, most particles would be monoclonal when <35% of the particles contain PCR products [23]. To confirm this, we annealed the aptamer particles with Cy5-labeled RP in binding buffer at 60°C for 10 minutes and cooled down at room temperature for 10 minutes. The particles were then washed twice with 100 μL binding buffer then analysed by flow cytometry. *Determining aptamer copy number on each AP:* Quantitative PCR (qPCR) was performed with a CFX384 Real-Time PCR detection system (Bio-Rad) to estimate the aptamer copy number for each AP. Calibration samples were prepared by adding 6×10, 6×10^2, 6×10^3, 6×10^4, 6×10^5, 6×10^6, 6×10^7, 6×10^8, or 6×10^9 templates into a 10 μL reaction containing 250 nM each of FP and RP, ~8,000 FP-coated particles, 5 μL GoTaq PCR Master Mix (Promega) and 0.5x SYBR green (Life Technologies). Test samples were prepared identically, but with ~10000 APs. From the threshold cycle, we quantified ~ 6×10^8 sequences on 10000 APs. Since only ~20% of APs displayed template sequences, the average copy number of sequences on each template-bearing AP was ~3×10^5.

Pro-SELEX screening. During Pro-SELEX screening, we incubated 5×10^7 aptamer particles with biotin-labelled MPO protein at different concentrations (see table S2 for detailed experimental conditions) in selection buffer (DPBS with 2.5 mM $MgCl_2$, 1 mM $CaCl_2$, 0.01% TWEEN-20, 0.2% BSA). To ensure the MPO molecules are not depleted during selection, reaction volumes were increased when using lower concentrations of the target. After 1 hour of incubation, the beads were washed three times with selection buffer. We then magnetically labeled the aptamer particle-captured MPO proteins by incubating the particles with 20 μL of anti-biotin microbeads (Miltenyi Biotech) in 1 mL of selection buffer for 15 min at room temperature. The particles were then washed with binding buffer twice and sorted by Pro-SELEX microfluidic devices. The aptamer particles captured at each capture zone of Pro-SELEX microfluidic devices were collected and stored at 4 °C.

High-throughput Sequencing. For each collected aptamer pool and the unsorted DNA pool, two rounds of PCR were performed to add adaptor sequences and sequencing indexes. The amplified sequences were then purified using agarose gel electrophoresis and PureLink™ Quick Gel Extraction Kit, quantified using a NanoDrop spectrophotometer, and sent to McMaster Genomics Facility for sequencing on an Illumina MiSeq.

Bioinformatics. Raw sequencing data was processed using Illumina's Basespace online platform to sort tagged sequence pools and output sequence data in FASTQ format. Paired-end reads were merged using USEARCH (v10)[45] and the primers were then trimmed using Cutadapt (V3.5)[46]. Sequences containing less than perfect complementarity were discarded to minimize sequencing errors in the dataset. FASTA format trimmed sequences were dereplicated and tagged with copy number using USEARCH. Read counts were then generated in the format of tab-delimited text files. The files were processed by the AptaZ script written in MATLAB (Version 2021a, MathWorks, US) to calculate the corresponding Z score for each sequence. Calculated Z scores were exported as CSV files for visualization and validation. The source code of AptaZ is available free of charge from the content associated with the article upon paper acceptance.

Affinity measurement. After sequencing analysis, we performed particle PCR to synthesize APs displaying each unique aptamer candidate sequence. Each particle PCR reaction (100 µL) consisted of 1x GoTaq PCR Master Mix (Promega), 25 mM $MgCl_2$, 2 µM phos-RP, 10 nM aptamer template and 5×10^6 FP-coated particles. PCR was carried out under the following cycling conditions: 94 °C for 3 min, followed by 30 cycles of 94 °C for 15 sec, 58 °C for 30 sec and 72 °C for 30 sec. To avoid particle aggregation and increase particle PCR efficiency, we vortexed the reaction every four cycles after the 94 °C denaturing step. We then removed the reverse strands using Lambda exonuclease as described above. We then incubated 1 µL of the APs with Cy5-RP and measured AP fluorescence intensity using flow cytometry to test particle PCR efficiency. For affinity measurement, different concentrations of biotinylated MPO (10 pM to 200 nM) were incubated with a fixed amount of the APs (2×10^4 particles) in selection buffer for 1 hr at room temperature. The unbound MPO was washed away with selection buffer, after which streptavidin-labeled Cy5 was introduced and incubated for 15 minutes to label the bound MPO. The particles were washed with binding buffer and median fluorescence intensities were quantified via flow cytometry and FlowJo software (version 10.8.1, FlowJo).

Data Availability.

The main data supporting the results in this study are available within the paper and its supplementary information. The source data underlying Figs. 1d, e, 2c, d, h, i, j, 3b, c, e, f, g, 4b, c, and Supplementary Figs 4, 5, 6, 10, 11, 12 are provided as a Source Data file.The sequencing data files are too large to be publicly shared, but they are available from the corresponding author upon reasonable request. The chip design (in the format of STL) and running protocol of the microfluidic chip will be available free of charge from the publisher's website as a supplementary file.

Code Availability

The code corresponding to the AptaZ algorithm can be accessed at https://github.com/dwangnu/AptaZ.

Methods-only references

44. Wang, Z. *et al.* Ultrasensitive and rapid quantification of rare tumorigenic stem cells in hPSC-derived cardiomyocyte populations. *Science Advances* **6**, (2020).

45. Edgar, R. C. & Bateman, A. Search and clustering orders of magnitude faster than BLAST. *Bioinformatics* **26**, 2460–2461 (2010).

46. Martin, M. Cutadapt removes adapter sequences from high-throughput sequencing reads. *EMBnet J* **17**, 10–12 (2011).

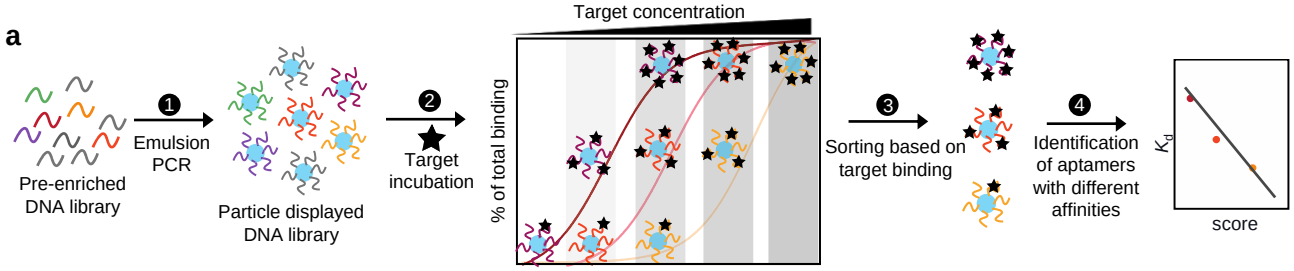
a
Pre-enriched DNA library
1
Emulsion PCR
Particle displayed DNA library
2
Target incubation
Target concentration
% of total binding
3
Sorting based on target binding
4
Identification of aptamers with different affinities
K_d
score

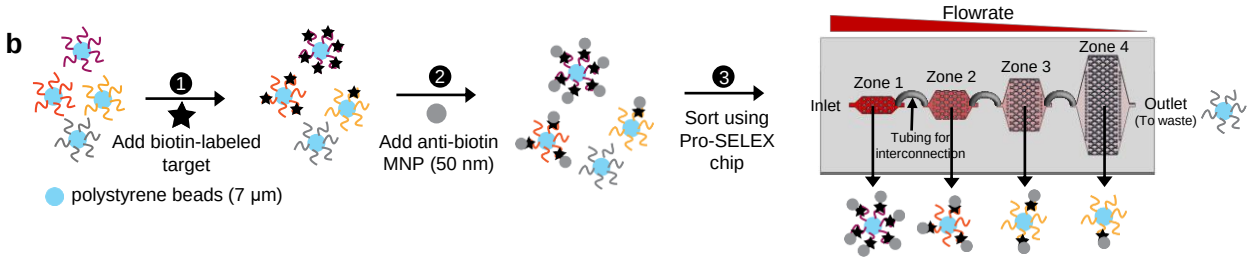
b
1
Add biotin-labeled target
polystyrene beads (7 μm)
2
Add anti-biotin MNP (50 nm)
3
Sort using Pro-SELEX chip
Flowrate
Inlet
Zone 1
Zone 2
Zone 3
Zone 4
Tubing for interconnection
Outlet
(To waste)

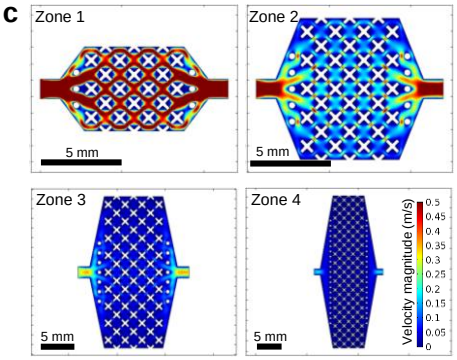
c
Zone 1
Zone 2
Zone 3
Zone 4
5 mm
Velocity magnitude (m/s)

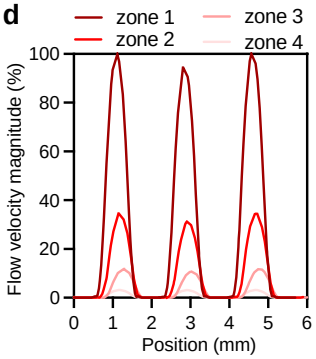
d
zone 1
zone 2
zone 3
zone 4
Flow velocity magnitude (%)
Position (mm)

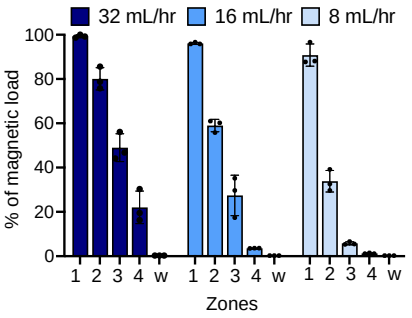
e
32 mL/hr
16 mL/hr
8 mL/hr
% of magnetic load
Zones

Figure 2.

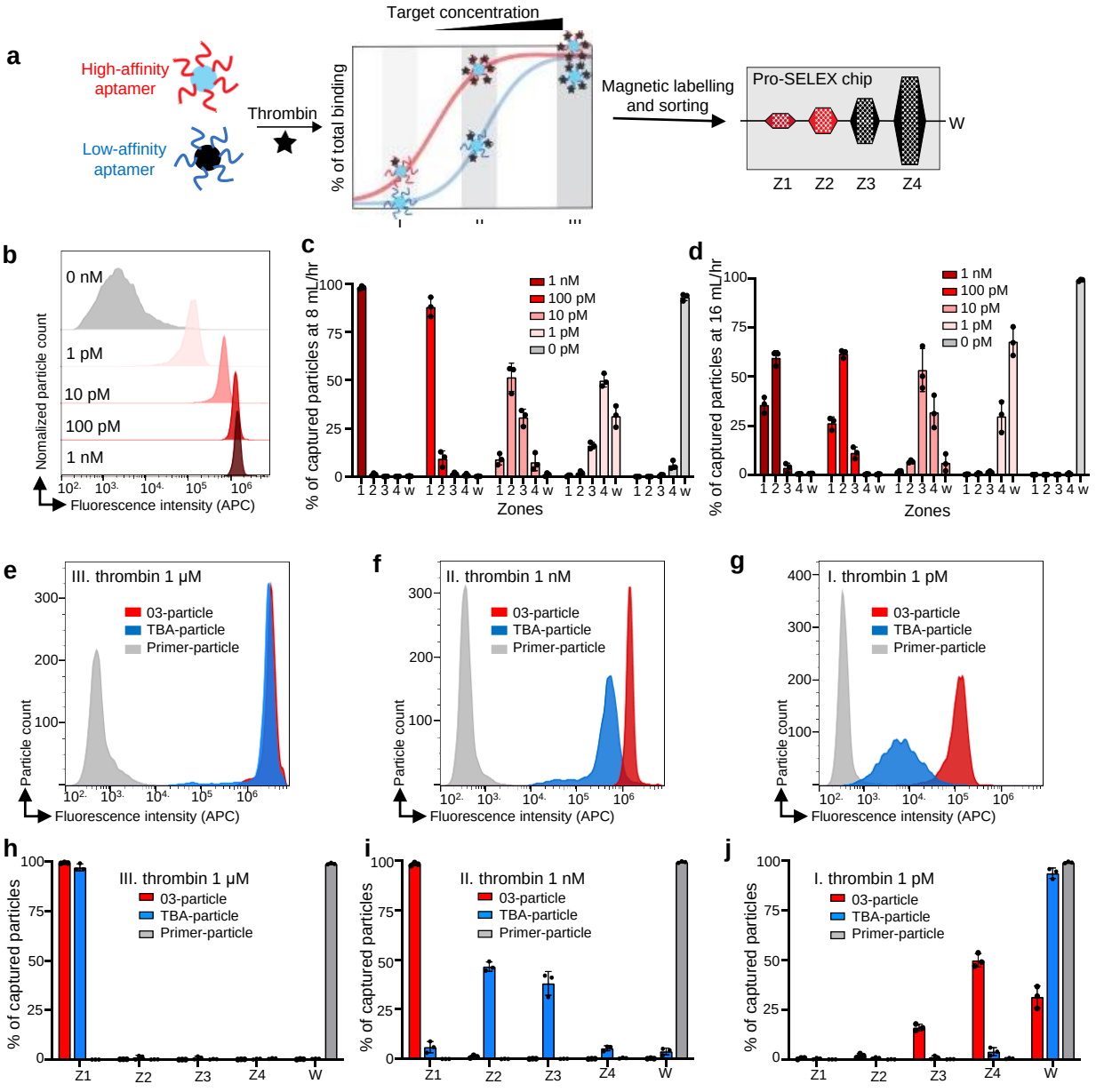
a
High-affinity aptamer
Low-affinity aptamer
Thrombin
Target concentration
% of total binding
I
II
III
Magnetic labelling and sorting
Pro-SELEX chip
Z1
Z2
Z3
Z4
W
b
0 nM
1 pM
10 pM
100 pM
1 nM
Nomalized particle count
Fluorescence intensity (APC)
c
% of captured particles at 8 mL/hr
1 nM
100 pM
10 pM
1 pM
0 pM
Zones
d
% of captured particles at 16 mL/hr
Zones
e
III. thrombin 1 μM
03-particle
TBA-particle
Primer-particle
Particle count
Fluorescence intensity (APC)
f
II. thrombin 1 nM
g
I. thrombin 1 pM
h
% of captured particles
i
II. thrombin 1 nM
j
I. thrombin 1 pM

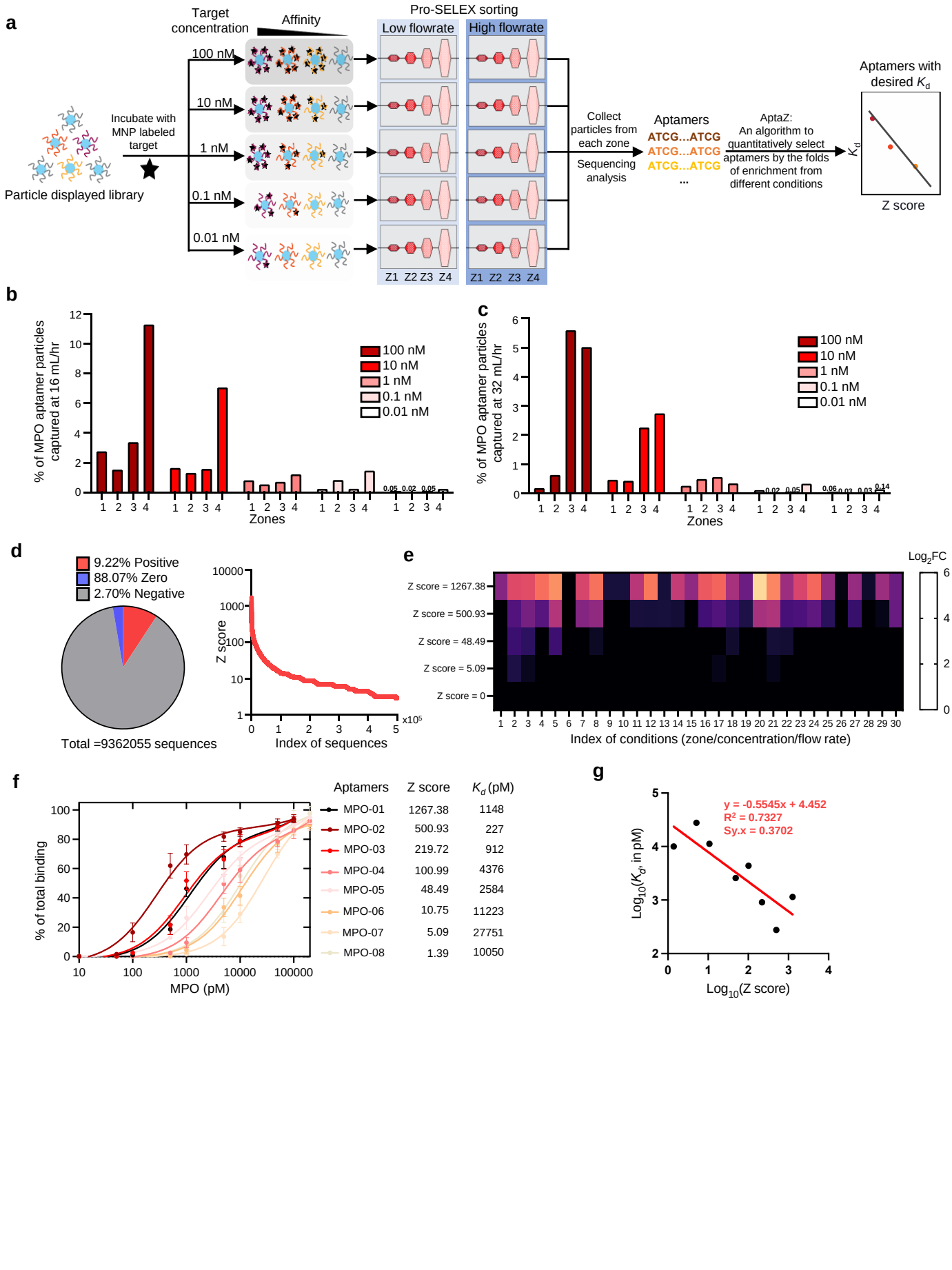
a
Target concentration
Affinity
Pro-SELEX sorting
Low flowrate
High flowrate
100 nM
10 nM
1 nM
0.1 nM
0.01 nM
Incubate with MNP labeled target
Particle displayed library
Z1 Z2 Z3 Z4
Collect particles from each zone
Sequencing analysis
Aptamers
ATCG...ATCG
ATCG...ATCG
ATCG...ATCG
...
AptaZ: An algorithm to quantitatively select aptamers by the folds of enrichment from different conditions
Aptamers with desired K_d
K_d
Z score
b
% of MPO aptamer particles captured at 16 mL/hr
100 nM
10 nM
1 nM
0.1 nM
0.01 nM
Zones
c
% of MPO aptamer particles captured at 32 mL/hr
Zones
d
9.22% Positive
88.07% Zero
2.70% Negative
Total =9362055 sequences
Z score
Index of sequences
e
Z score = 1267.38
Z score = 500.93
Z score = 48.49
Z score = 5.09
Z score = 0
Log2FC
Index of conditions (zone/concentration/flow rate)
f
% of total binding
MPO (pM)
Aptamers
Z score
K_d (pM)
MPO-01 1267.38 1148
MPO-02 500.93 227
MPO-03 219.72 912
MPO-04 100.99 4376
MPO-05 48.49 2584
MPO-06 10.75 11223
MPO-07 5.09 27751
MPO-08 1.39 10050
g
y = -0.5545x + 4.452
R² = 0.7327
Sy.x = 0.3702
Log10(K_d, in pM)
Log10(Z score)

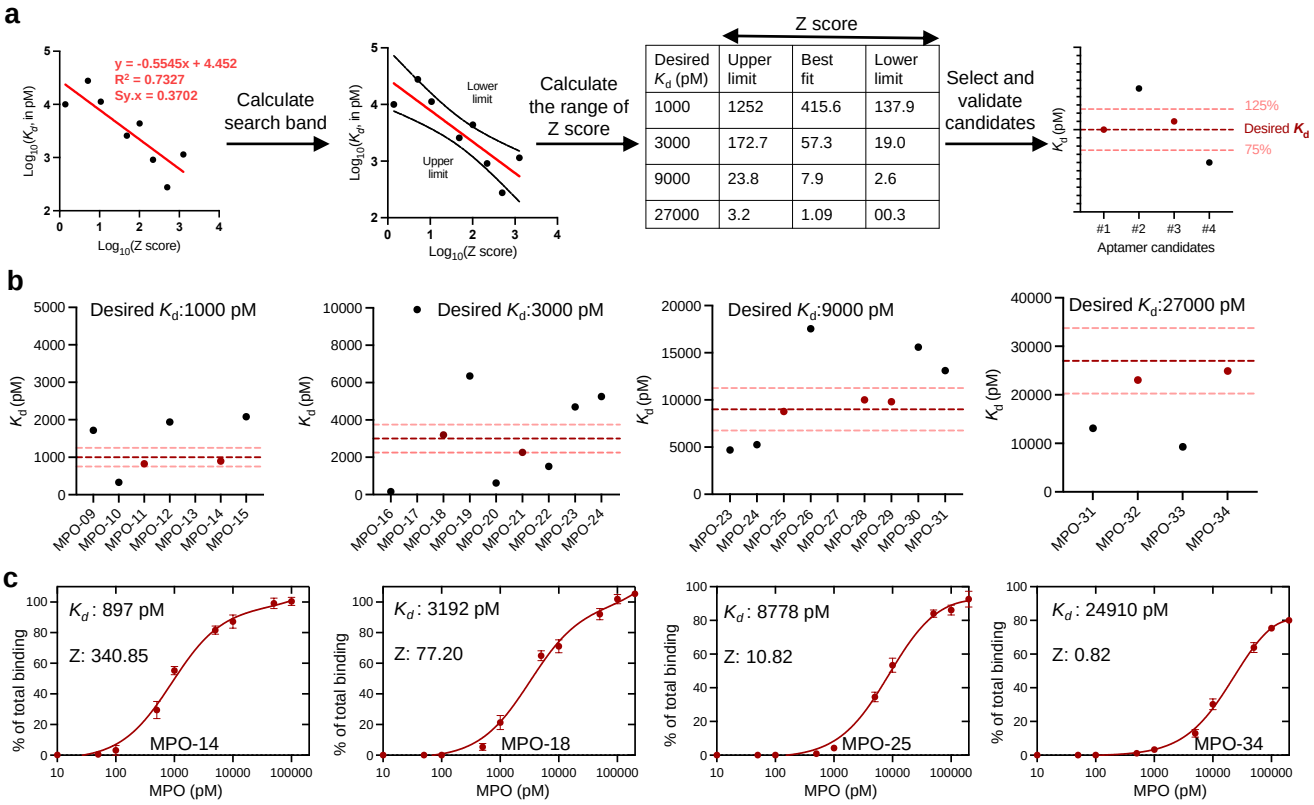
a
y = -0.5545x + 4.452
R² = 0.7327
Sy.x = 0.3702
Log10(Kd, in pM)
Log10(Z score)
Calculate search band
Lower limit
Upper limit
Calculate the range of Z score
Z score
Desired Kd (pM)
Upper limit
Best fit
Lower limit
1000
1252
415.6
137.9
3000
172.7
57.3
19.0
9000
23.8
7.9
2.6
27000
3.2
1.09
00.3
Select and validate candidates
125%
Desired Kd
75%
#1
#2
#3
#4
Aptamer candidates
b
Desired Kd:1000 pM
Desired Kd:3000 pM
Desired Kd:9000 pM
Desired Kd:27000 pM
Kd (pM)
MPO-09
MPO-10
MPO-11
MPO-12
MPO-13
MPO-14
MPO-15
MPO-16
MPO-17
MPO-18
MPO-19
MPO-20
MPO-21
MPO-22
MPO-23
MPO-24
MPO-23
MPO-24
MPO-25
MPO-26
MPO-27
MPO-28
MPO-29
MPO-30
MPO-31
MPO-31
MPO-32
MPO-33
MPO-34
c
Kd: 897 pM
Z: 340.85
MPO-14
Kd: 3192 pM
Z: 77.20
MPO-18
Kd: 8778 pM
Z: 10.82
MPO-25
Kd: 24910 pM
Z: 0.82
MPO-34
% of total binding
MPO (pM)

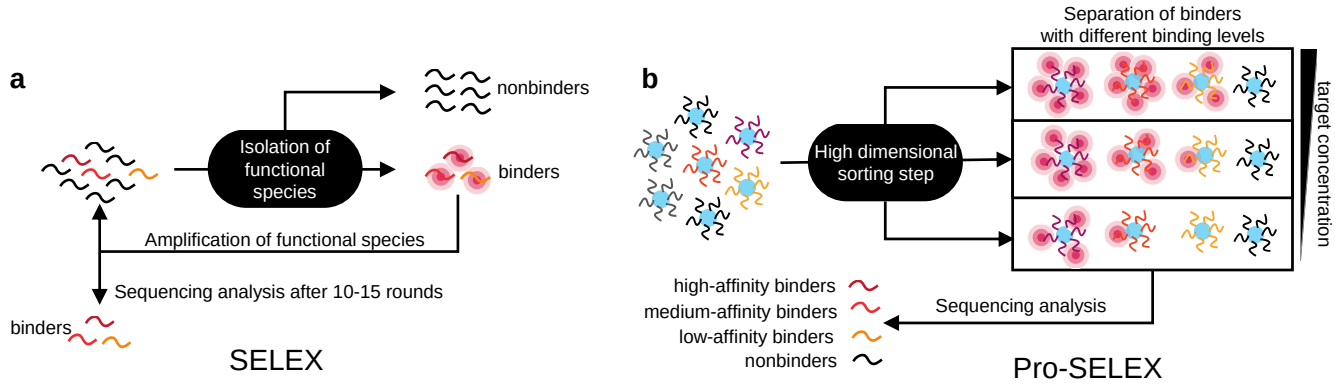

c

Aptamer selection technologies	Pro-SELEX	SELEX[16,18,19]	Particle display[23]	CE-SELEX[20]
Rounds required	1 (3 pre-enrichment rounds)	10-15	3-5 (3 pre-enrichment rounds)	1-5
Programmable affinity?	K_d is programmable within dynamic testing range	Not programmable	K_d is programmable, but only for high-affinity aptamers	Not programmable
Throughput	High (multiple conditions in one round)	Low (1 condition in each round)	Low (1 condition in each round)	Low (1 condition in each round)

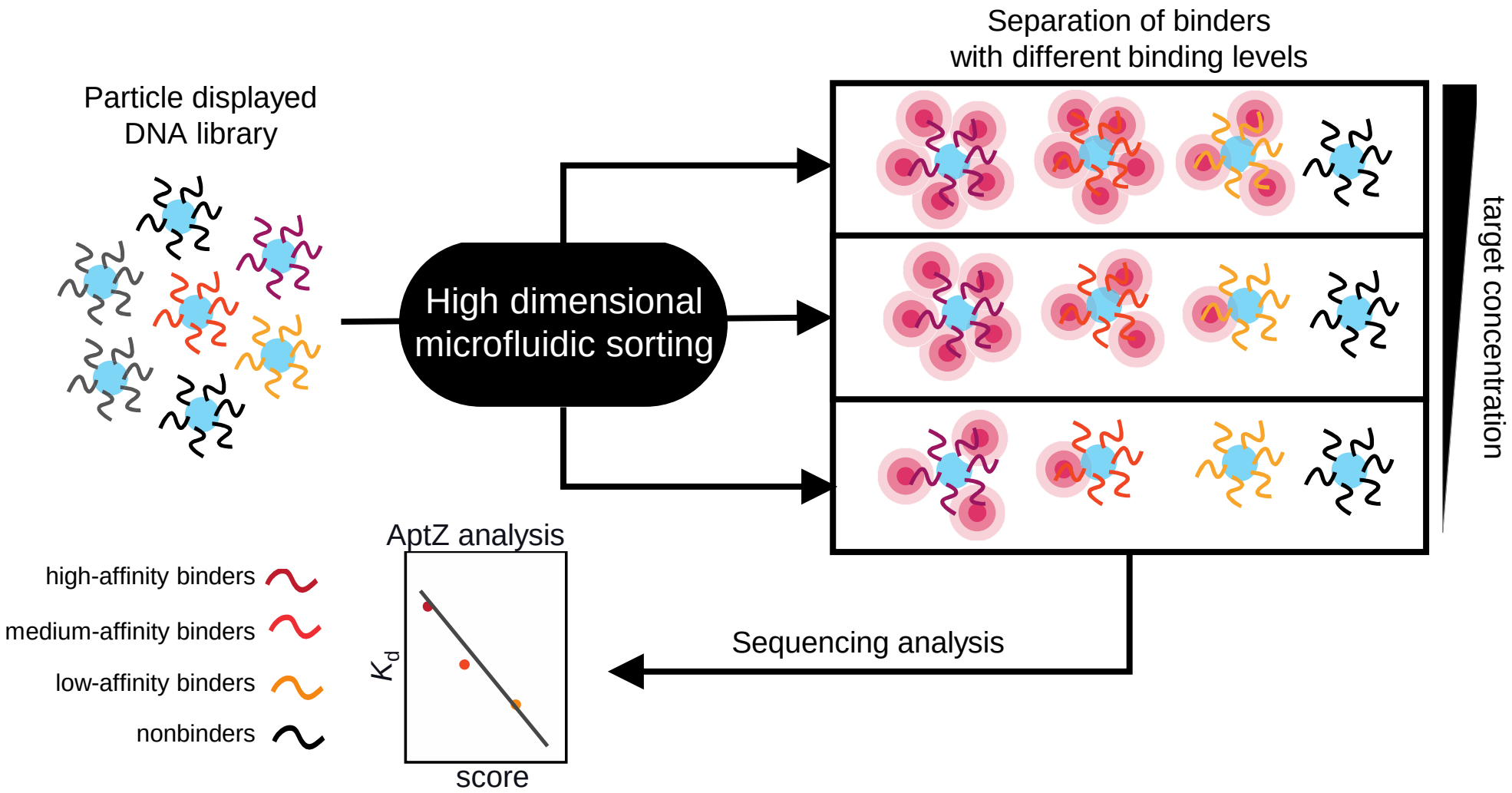
Separation of binders
with different binding levels
Particle displayed
DNA library
High dimensional
microfluidic sorting
target concentration
AptZ analysis
high-affinity binders
medium-affinity binders
low-affinity binders
nonbinders
K_d
score
Sequencing analysis